Life Sciences 324 (2023) 121746

Contents lists available at ScienceDirect

Life Sciences

journal homepage: www.elsevier.com/locate/lifescie

Novel insights and mechanisms of diet-induced obesity: Mid-term *versus* long-term effects on hepatic transcriptome and antioxidant capacity in Sprague-Dawley rats

Alejandro García-Beltrán [a,1], Rosario Martínez [a,1], Jesus M. Porres [a,*], Francisco Arrebola [b], Inmaculada Ruiz Artero [b], Milagros Galisteo [c], Pilar Aranda [a], Garyfallia Kapravelou [a,1], María López-Jurado [a,1]

[a] Department of Physiology, Institute of Nutrition and Food Technology (INyTA), Centre for Biomedical Research (CIBM), Institute for Research in Sport and Health (IMUDS), Universidad de Granada, 18016 Granada, Spain
[b] Department of Histology, Institute of Neurosciences, Centre for Biomedical Research (CIBM), Universidad de Granada, 18016 Granada, Spain
[c] Department of Pharmacology, School of Pharmacy, Centre for Biomedical Research (CIBM), Universidad de Granada, Campus Universitario de Cartuja s/n, 18071 Granada, Spain

ARTICLE INFO

Keywords:
Obesity
Aging
Liver
Glucose & lipid metabolism
Antioxidant capacity
Rats

ABSTRACT

Aims: The study of molecular mechanisms related to obesity and associated pathologies like type 2-diabetes and non-alcoholic fatty liver disease requires animal experimental models in which the type of obesogenic diet and length of the experimental period to induce obesity deeply affect the metabolic alterations. Therefore, this study aimed to test the influence of aging along a rat model of diet-induced obesity in gene expression of the hepatic transcriptome.

Main methods: A high-fat/high-fructose diet to induce obesity was used. Mid- (13 weeks) and long-term (21 weeks) periods were established. Caloric intake, bodyweight, hepatic fat, fatty acid profile, histological changes, antioxidant activity, and complete transcriptome were analyzed.

Key findings: Excess bodyweight, hepatic steatosis and altered lipid histology, modifications in liver antioxidant activity, and dysregulated expression of transcripts related to cell structure, glucose & lipid metabolism, antioxidant & detoxifying capacity were found. Modifications in obese and control rats were accounted for by the different lengths of the experimental period studied.

Significance: Main mechanisms of hepatic fat accumulation were *de novo* lipogenesis or altered fatty acid catabolism for mid- or long-term study, respectively. Therefore, the choice of obesity-induction length is a key factor in the model of obesity used as a control for each specific experimental design.

1. Introduction

Nowadays, obesity and associated pathologies including non-alcoholic fatty liver disease (NAFLD), metabolic syndrome (MetS), and alterations in bone functionality, constitute an important burden for national health systems. The prevalence of these diseases is very high and the fact that life expectancy, as a result of the increase in obesity, could decrease for the first time in recent times has generated great alarm [1]. Due to their high prevalence in the world population, obesity and MetS are considered pandemics. This condition affects approximately 20–40 % of the population in industrialized nations, and its prevalence is expected to rise further in the next decades [2]. Their incidence increases alarmingly every year mainly due to environmental factors, although genetic factors are also involved [3]. Concerning environmental factors, energy imbalance is influenced by a diet high in saturated fat and refined sugars as well as a sedentary lifestyle [4]. The regular intake of high fat and high fructose diets is directly related to the development of obesity, which is an important risk factor for other

* Corresponding author at: Institute of Nutrition and Food Technology, Centre for Biomedical Research, Universidad de Granada, Avda. del Conocimiento S/N., Armilla 18016, Granada, Spain.
E-mail address: jmporres@ugr.es (J.M. Porres).
[1] These authors contributed equally to this work.

https://doi.org/10.1016/j.lfs.2023.121746
Received 21 February 2023; Received in revised form 8 April 2023; Accepted 25 April 2023
Available online 29 April 2023

associated chronic pathologies [3].

Experimental animal models are indispensable tools for the study of the alterations in morphology and metabolic pathways involved in the development of overweight and obesity. Although numerous models have been developed, they are usually classified into two main categories such as genetic or diet-induced obesity (DIO). Genetic models exhibit strong symptoms and can be associated with MetS or its hepatic manifestation, NAFLD. However, genetic obesity has a lower distribution compared to other forms of obesity that are more related to environmental factors. In this regard, DIO models may be closer to the actual situation that is more prevalent in the human population. DIO models are usually generated using a high-fat semi-synthetic diet (HFD) with either 60 or 45 % of the total caloric content present as fat [5,6], although cafeteria diets prepared with a mixture of ingredients representative of a western type diets (fried potatoes, biscuits, bacon, standard chow diet, pork pate base and liquid chocolate) are also used [7]. In recent years, and to resemble more accurately the consume trends by humans, the use of diets with 45 % of kcal present as fat in combination with a high mono or di-saccharide content (fructose or sucrose) has been recommended for DIO models [5,6]. Furthermore, other diet-related considerations present in the former diets should be considered like the presence of casein as the main protein source, which *per se* has been reported to induce significant alterations in rat's glucose and lipid metabolism [8]. Nevertheless, a general trend of outcomes may be described for most of the diet-induced obesity interventions that incorporate overweight, metabolic dysregulation or alterations in liver histology.

Likewise, another factor that should be considered when designing DIO models is the extensive length of time that is usually needed to implement such models and develop the adequate bodyweight and metabolic alterations sought. Such periods may lead to an aging process of the animals that will in turn significantly affect the extent to which different genes are expressed [9], and thus metabolic pathways are affected. The longer the experimental period implemented, the more extensive the damage in different organ functionality caused by the dietary conditions implemented to produce the development of obesity. All these changes are matched by a progressive functional decline in various organs over time, changes in the biotransformation of xenobiotics, and impairment of normal cellular functions by free radicals. Aged animals have altered activity of drug-metabolizing enzymes such as glutathione S-transferases [10], and aging is associated with down-regulated expression of genes related to antioxidant function, thus impairing the antioxidant capacity of the liver and increasing oxidative damage in old animals [11]. Moreover, the adaptation of key transcription factors involved in lipid metabolism in response to nutritional status changes is impaired in old rats, and this might contribute to the development of hepatic steatosis with aging [12]. In the liver of Wistar rats, aging caused an increase in the mRNA abundance of lipogenic transcription factors and enzymes, and a decrease in mRNA levels of enzymes associated with mitochondrial fatty acid oxidation such as carnitine-palmitoyl transferase-1 (CPT-1a) [11].

In this experiment, we have developed an animal model of diet-induced obesity (DIO) using a HFD (45 % of total dietary Kcal) and refined sugars (20 % fructose solution) to resemble the events that take place in the human population. 10-week-old male Sprague-Dawley rats were used and fed *ad libitum* during 13 or 21 weeks with an unbalanced high-fat high-fructose diet that produces a pathological state similar to human obesity. Specifically, we aimed to (i) develop a rat experimental model of obesity and non-alcoholic fatty liver disease along two different maturity stages of the experimental animals, (ii) perform an *in vivo* study of hepatic transcriptome profile and detection of the main markers associated with NAFLD, and (iii) test the influence of aging along DIO in potential metabolic and histological damage, as well as in gene expression of hepatic transcripts related to cell structure components, glucose and lipid metabolism, or antioxidant and detoxifying defense system.

2. Material and methods

2.1. Chemical compounds

Cumene hydroperoxide, KCN, 2,3-bis-(2-methoxy-4-nitro-5-sulfophenyl)-2H-tetrazolium-5-carboxanilide (XTT), dichlorophenolindophenol (DCIP), flavin adenine dinucleotide (FAD), 1-chloro-2,4-dinitrobenzene (CDNB), NADPH, xanthine, xanthine oxidase, reduced glutathione, and sodium azide were from Sigma-Aldrich (Madrid, Spain). Diethylene triamine pentaacetic acid (DETAPC) was from Panreac Applichem (Barcelona, Spain).

2.2. Animals and experimental design

A total of 32 male Sprague-Dawley rats (Charles River, Barcelona) were housed in group cages with solid-bottom and nest shavings (4 rats in each cage), and located in a well-ventilated, thermostatically controlled room (21 ± 2 °C) under a 12-h light/dark cycle to ensure animal welfare (Unidad de Experimentación Animal, CIC, University of Granada). After a week of acclimatization, animals aged 10 weeks with a starting average body weight of 357 ± 2 g, were randomly divided into four experimental groups of eight animals per group. All the cages in each specific experimental group were labeled accordingly and placed in order to avoid possible identification errors. All the researchers and animal facility personnel were trained to ensure the correct identification of cages in each experimental group. The handling of the animals was refined to the minimum necessary to ensure their comfort during the experiments and to avoid causing unnecessary stress.

Two groups of animals consumed a standard diet (20 % kcal protein, 10 % kcal fat) (TD.08806, ENVIGO, Madison, WI) for 13 or 21 weeks (SD1 and SD2, respectively) while the remaining two experimental groups consumed a HFD (19 % kcal protein, 45 % kcal fat) (TD.06415, ENVIGO, Madison, WI) and were fed 20 % fructose in the drinking water for 13 or 21 weeks (HFHF1 and HFHF2, respectively) since the combination of high fat and high fructose generates a higher weight gain, hyperinsulinemia, hepatic steatosis and oxidative stress than a high fat, low-carbohydrate diet [5,6] and promotes *de novo* lipogenesis and the aggravation of glucose and fat metabolism disorders [6]. During the experimental period, the animals had free access to fluid (water or 20 % fructose solution), and animals of the HFD group consumed the experimental diet *ad libitum*, while the animals of the standard-diet group followed a *pair-fed* design of food consumption based on previous experiments [9] to maintain adequate caloric intake in a normocaloric group. Food intake was recorded daily whereas bodyweight was measured weekly. All experiments were undertaken according to Directional Guides Related to Animal Housing and Care [13], and all procedures were approved by the Animal Experimentation Ethics Committee of the University of Granada, Spain (Project Reference 16/07/2019/132). To select the number of rats assigned to each experimental group (n = 8), we implemented the 3Rs principle [14]. General health monitoring of all animals was performed every day. Criteria for the health monitoring include wound, bleeding, hair brilliance, nasal discharge, eye discharge, convulsions, alterations in heart rate, anal and genital discharge, and general motor activity. An end point criterion was established if the animals suffered any type of physical damage, showed symptoms of anorexia with a decrease in intake of 30 % or more, or weight loss of 25 % or more. If, based on the manifestations presented by the animal, it is decided that it is in an irreversible state of suffering, the experimental death of the specific animal is declared, and its sacrifice is considered, in case it should be necessary.

No adverse effect derived from the obesity induction was observed in the experimental animals at either length of the experimental period. In addition, no animal became severely ill or died before the experimental endpoints. At the end of the 13- or 21-week experimental period, the animals were anesthetized with ketamine (75 mg·kg^{-1} body weight) and xylazine (10 mg·kg^{-1} body weight), and blood was collected by

abdominal aorta puncture using heparin as an anticoagulant. The liver was extracted, weighed, divided into various portions and immediately frozen in liquid nitrogen and stored at −80 °C except for 100 mg that were immersed in RNA preserving solution (RNAlater, Ambion).

2.3. Total hepatic lipid content

A liver portion was lyophilized to assess the moisture content. Hepatic lipids were extracted using hexane from an aliquot of the freeze-dried liver portion using the method described by Folch et al. [15] with the modifications made by Kapravelou et al. [16]. Total liver lipids were measured gravimetrically after solvent extraction under N_2 stream.

2.4. Microscopic liver study

A portion of the liver was fixed in 10 % phosphate-buffered formalin, dehydrated in ethanol, embedded in paraffin, and sectioned for histological examination using hematoxylin-eosin (HE) staining for general microscopy morphology (Servicio de Microscopía, CIC, University of Granada). Eight animals were evaluated per experimental group (n = 32 samples per group) and four different preparations of each staining were analyzed for each animal. Histological alterations were evaluated in zones 1, 2, and 3 of the acinus. For semi-quantitative evaluation of liver damage, an initial scoring was done using the Brunt evaluation based on the following parameters: macrovesicular steatosis, microvesicular steatosis, ballooning, periportal inflammation, centrilobular inflammation, and fibrosis. For the semi-quantitative evaluation, the following cross-scale was used: (−) non-existent, (+) mild, (++) mild-moderate, (+++) moderate, (++++) severe [17]. In case of differences among treatments being found in the Brunt evaluation, the Non-Alcoholic Steatohepatitis (NASH) semi-quantitative scoring system of Kleiner et al. [18] as adapted by Chen et al. [19] was used to evaluate the degree of NASH development following the recommendations of Martinez et al. [9]. The scoring system comprised 14 histological features, 4 of which were evaluated semi-quantitatively: steatosis (0–3), lobular inflammation (0–2), hepatocellular ballooning (0–2), and fibrosis (0–4). Another nine features were recorded as present or absent. NAS score was calculated by the sum of steatosis grade, lobular inflammation, and ballooning. NAS of >5 correlated with a diagnosis of "NASH", and scores of <3 were diagnosed as "not NASH" [18].

2.5. Fatty acid profile of the liver

A freeze-dried liver portion was extracted and methylated according to Lepage and Roy [20] for gas chromatography analysis of fatty acid profile using an Agilent 7890A chromatograph equipped with CTC Pal combi-xt model sampler and a Waters Quattro micro GC mass spectrometer detector. Individual fatty acid methyl esters (FAMEs) were separated with a 30 × 0.25 mm ZB Fame capillary column (0.2 μm thickness) (Phenomenex, Torrance, CA, USA). The gas chromatography conditions were as follows: injector temperature 250 °C, injection volume 2 μL Split (proportion 10:1), temperature gradient from 100 °C to 210 °C with a rate of 4 °C/min, hold time 5 min. The flow rate of the carrier gas (Helium) was 1 mL/min. The analysis time was 40 min and the measurement range 45–450 uma (scan mode). Chromatographic data were recorded and integrated using Masslynx, version 4.1 software. FAMEs were identified using analytical standards and mass spectral library. Peak areas were measured and used to calculate the percentage of each fatty acid related to the total sum of all the fatty acid areas in the sample. Furthermore, some products-to-precursor fatty acid ratios were used as indices of desaturase or desaturase-elongase enzyme activities in the liver as described by Gonzalez-Torres et al. [21] using the following formulas.

Delta-6-elongase-desaturase activity:

(i) docosahexaenoic acid/linolenic acid

(ii) arachidonic acid/linoleic acid

Stearoyl-CoA activity (SCD):

(i) palmitoleic acid/palmitic acid
(ii) oleic acid/stearic acid

Delta-5 desaturase activity:

(i) arachidonic acid/eicosatrienoic acid

2.6. RNA extraction

Total RNA was isolated from the liver of all rats in each experimental group (n = 8/group). One hundred milligrams of tissue were homogenized in 1 mL of Tri-Reagent® (Sigma-Aldrich). The RNA was solubilized in RNAse-free H_2O and treated with DNase (Applied Biosystems) to remove any DNA present in the sample.

2.7. Transcriptomics

For hepatic transcriptomics analysis, six total-RNA samples per experimental group were randomly selected. Library preparation and Illumina sequencing were carried out at the IPBLN Genomics Facility (CSIC, Granada, Spain). Total RNA quality was verified by Bioanalyzer RNA 6000 Nano chip electrophoresis (Agilent Technologies). Every RNA sample showed a RIN value above 8.4. RNA-seq libraries were prepared using Truseq stranded mRNA kit (Illumina®) from 200 ng of input total RNA. Quality and size distribution of PCR-enriched libraries were validated through Bioanalyzer High Sensitivity DNA assay and concentration was measured on the Qubit® fluorometer (Thermo). Final libraries were pooled in an equimolecular manner and then diluted and denatured as recommended by Illumina NextSeq 500 library preparation guide. The 75 × 2 nt paired-end sequencing was conducted on a NextSeq 500 sequencer with a final output of 70 Gbp and a quality score (Q30) of 97 %. The reads from Illumina paired-end sequencing were quality-checked using FastQC v0.11.9 [22] and MultiQC v1.9 [23]. It was verified that throughout the sequence of the reads, their average quality presented a Phred nitrogen base quality score >30, so it was not necessary to filter the data. Then, the mapping of the reads was carried out. For this, HISAT2 v2.2.1 was used [24]. The *Rattus norvegicus* genome obtained from Ensembl (Rattus_norvegicus.Rnor_6.0.dna.toplevel.fa file) was chosen as the reference genome for alignment and the reads. The SAM files resulting from these mappings were ordered, transformed into BAM files, and indexed, all using SAMtools v1.10 [25]. In the next step, the count of the reads that mapped against each of the genes was carried out, for which the BAM files obtained in the previous step, the annotation file in GTF format of the reference genome (accession GCA_000001895. 4), and the feature counts v2.0.1 [26] were used. Finally, differential expression analysis was performed using the count tables obtained in the previous step and the programs DESeq [27], DESeq2 [28], and edgeR [29]. Transcripts were defined as differentially expressed when the fold change (FC) between the groups (SD1, HFHF1, SD2, HFHF2) was >1.3 (percentage of change +30 %; upregulated) or <−1.3 (percentage of change −30 %; downregulated) and the *P*-value of the Student's *t*-test was <0.05. Identical or similar filter criteria were used in several recent studies [30,31].

2.8. RNA extraction and quantitative RT-PCR

To validate the transcriptomic analysis, targeted gene expression was conducted using RT-PCR. A total of 100–250 ng of RNA was reverse-transcribed according to standard protocols using a Lifepro Thermal Cycler (Bioer Serves Life, P. R. China). Quantitative RT-PCR was performed with QuantStudio 12 K Flex Real-Time PCR System (Applied Biosystems), using primers for genes involved in cell structure, glucose

& lipid metabolism, and antioxidant & detoxifying capacity (Table 1). The PCR master mix reaction included the first strand cDNA template, primers, and 2× TaqMan® Fast Universal PCR Master Mix, No AmpErase® UNG (Applied Biosystems). Expression of the test gene was related to that of *Actb* reference measured in parallel in the same sample using the ΔCt method. The $2^{-\Delta\Delta Ct}$ method was used to analyze the data in reference to the control group.

2.9. Antioxidant and detoxifying enzymes activity assays

A fresh liver aliquot was homogenized (1:10 w/v) in 50 mM phosphate buffer (pH 7.8) containing 0.1 % Triton X-100 and 1.34 mM diethylene triamine pentaacetic acid (DETAPAC) using a Micra D-1 homogenizer (ART moderne labortechnik) at 18,000 rpm for 30 s followed by treatment with a Sonoplus HD 2070 ultrasonic homogenizer (Bandelin) at 50 % power three times for 10s. Liver homogenates were centrifuged at 13,000 ×*g*, 45 min, 4 °C, and the supernatant was used to determine the activity of antioxidant enzymes. Catalase (CAT) activity was measured by the method of Cohen et al. [32] and expressed as enzyme units calculated by the following formula: ln(A1/A2)/t, where ln is the natural log, A1 and A2 are the observed absorbances at the two selected time points, and t is the reaction time between the two points. Total Glutathione Peroxidase (GPx) activity was determined by the coupled assay of NADPH oxidation [33] using cumene hydroperoxide as a substrate. The enzyme unit was defined as nmol of NADPH oxidized per min. Total superoxide dismutase (SOD) activity was measured as described by Ukeda et al. [34]. Mn-SOD activity was determined by the same method after treating the samples with 4 mM KCN for 30 min. CuZn-SOD activity resulted from subtracting the Mn-SOD activity from the total SOD activity. One unit of SOD activity was defined as the enzyme needed to inhibit 50 % 2,3-bis-(2-methoxy-4-nitro-5-sulfophenyl)-2H-tetrazolium-5-carboxanilide (XTT) reduction. NADH: Quinone reductase (QR) activity was determined according to the method of Ernster [35] using dichlorophenolindophenol (DCIP) and flavin adenine dinucleotide (FAD) as electron acceptor and inhibitor, respectively. The activity was expressed as enzyme units per min. The glutathione S-transferase (GST) was assayed by the method of Habig et al. [36], employing 1-chloro-2,4-dinitrobenzene (CDNB) as substrate, and expressed as enzyme units per min. The protein concentration was assayed by the method of Bradford [37].

2.10. Statistical analysis

The effects of dietary intervention with HFHF *vs* SD, and length of the experimental period as a measure of aging (13 *vs* 21 weeks) on hepatic weight, total fat content, fatty acid profile and indices, and antioxidant or detoxifying enzyme activity were analyzed by 2 × 2 factorial ANOVA, with dietary intervention and length of the experimental period as main treatments. The use of 2 × 2 factorial ANOVA is based on the potential interactions among the two interventions assayed (high-fat high-fructose diet, length of experimental period) being significant in our statistical model in addition to single effects. To reinforce the potential integrative strength of the statistical model implemented, the R^2 statistic has been included in the tables as a measure of the goodness of fit of the model, given that the coefficient of determination indicates the proportion of variability in a data set that can be accounted by the statistical model. Results are given as mean values and pooled SEM. Duncan's test was used to detect differences between treatment means. Differences were considered significant at $P < 0.05$. Model assumptions were checked using the Shapiro-Wilk normality test and Levene's test for homogeneity of variance, and by visual inspection of frequency histogram, quantile-quantile plot, and residual and fitted value plots. Pearson's test was carried out on the different antioxidant & detoxifying enzyme data to test the correlation between the transcript expression and enzymatic activity; when Pearson's test showed $r > 0.4$ and $P < 0.05$, results were considered statistically significant. SPSS v.25 was used for the statistical treatment. Student's t-test was used to detect differences in fold change of transcript expression between the control and experimental groups (SD1, HFHF1, SD2, HFHF2).

Table 1
Gene distribution in categories for expression study.

Function		Gen	Protein	Assay ID (Applied biosystems)
Cell structure	Anatomic cell structure	*Mmp15*	Matrix metalloproteinase-15	Rn01536925_m1
		Psmb9	Proteasome subunit beta type-9	Rn00680664_g1
	Cell adhesion	*Col26a1*	Collagen alpha-1(XXVI) chain	Rn01499402_m1
	Cell damage	*Cdkn1a*	Cyclin-dependent kinase inhibitor 1	Rn00589996_m1
		Gadd45a	Growth arrest and DNA damage-inducible protein alpha	Rn01425130_g1
	Cell proliferation	*Gdf15*	Growth/differentiation factor 15	Rn00570083_m1
		Myc	Myc proto-oncogene protein	Rn00561507_m1
	Solute transport	*Abcg5*	ATP-binding cassette sub-family G member 5	Rn01499073_m1
		Slc2a2	Solute carrier family 2, facilitated glucose transporter member 2	Rn00563565_m1
		Slc34a2	Sodium-dependent phosphate transport protein 2B	Rn00584515_m1
Glucose & lipid metabolism	Lipogenic action	*Agpat3*	1-acyl-sn-glycerol-3-phosphate acyltransferase gamma	Rn01428234_m1
		Fabp5	Fatty acid-binding protein 5	Rn01461858_g1
		Fasn	fatty acid synthase	Rn00569117_m1
		Pnpla3	Patatin-like phospholipase domain-containing protein 3	Rn01502361_m1
		Scd1	stearoyl-CoAdesaturase-1	Rn00594894_g1
		Srebf1	Sterol regulatory element binding transcription factor 1	Rn01495769_m1
		Pparg	Peroxisome proliferator-activated receptor gamma	Rn00440945_m1
	Lipolytic action	*Cpt1a*	Carnitine palmitoyl transferase 1A	Rn00580702_m1
		Crot	Peroxisomal carnitine O-octanoyltransferase	Rn01526940_m1
		Ppara	Peroxisome proliferator activated receptor alpha	Rn00566193_m1
	Cholesterol metabolism	*Cyp1a1*	Cytochrome P450 1A1	Rn01418021_g1
		Cyp1a2	Cholesterol 25-hydroxylase	Rn00561082_m1
		Cyp7a1	Cholesterol 7 alpha-hydroxylase	Rn00564065_m1
		Hmgcr	3-hydroxy-3-methylglutaryl-coenzyme A reductase	Rn00565598_m1
	Glucose metabolism	*Gck*	Hexokinase-4	Rn00688285_m1
Antioxidant & detoxifying capacity		*Akr7a3*	Aflatoxin B1 aldehyde reductase member 3	Rn00680664_m1
		Gpx1	Glutathione peroxidase 1	Rn00577994_g1
		Nfe2l2	nuclear factor erythroid 2 like 2	Rn00477784_m1
		Nqo1	NAD(*P*)H:quinone oxidoreductase 1	Rn00566528_m1
		Sod1	Superoxide dismutase [Cu-Zn]	Rn00566938_m1
		Ucp2	Mitochondrial uncoupling protein 2	Rn01754856_m1

3. Results

3.1. Food, fluid, caloric intake, and bodyweight gain

The influence of dietary treatment (SD or HFHF) and length of the experimental period (13 or 21 weeks) on food, fluid, caloric intake, and bodyweight gain of rats are shown in Fig. 1A–D. There was a marked dietary treatment effect on food intake derived from the higher amount of food consumed throughout the experimental period by rats on the standard diet (SD) compared to animals on the high-fat diet (HFHF) groups. In contrast, caloric and fluid intake was higher in rats fed HFHF along the entire experimental period *vs* SD-fed animals. Such differences led to greater bodyweight gain in rats that consumed the HFHF *vs* SD diet.

3.2. Liver weight and hepatic fat content

Dietary treatment with a high-fat high-fructose diet (HFHF1, HFHF2) had a significant effect on both liver weight and total hepatic fat content (Fig. 2), which exhibited higher values in the former groups compared to those treated with the SD diet. The length of the experimental period significantly affected the amount of total liver fat in HFHF groups, resulting in greater values for that parameter at 21 *vs* 13 weeks.

3.3. Liver histological study

Liver histological changes resulting from DIO along 13 or 21 weeks of experimental period are described in Figs. 3A–C and Supplemental Tables S1 and S2. Animals on the SD or HFHF dietary treatments for 13 weeks exhibited mild to moderate hepatic steatosis, mainly microvesicular, with a low degree of macrovesicular steatosis or cell ballooning (Fig. 3A–B). In the SD experimental group, between 33 and 66 % of rats exhibited steatosis, whereas that percentage raised to >66 % in the animals of the HFHF group (Supplementary Table S1). Conversely, rats fed for 21 weeks with the SD diet exhibited a similar degree of steatosis (33–66 %), but a lower extent of microvesicular and slightly higher macrovesicular changes. Between 33 and 66 % of the rats in the 21-week HFHF experimental group showed steatosis. However, macrovesicular changes experienced a marked increase at the expense of microvesicular steatosis, whereas a significantly higher number of hepatocytes showed clear signs of ballooning. Interestingly, macrovesicular steatosis took place mainly on the convex area of the selected

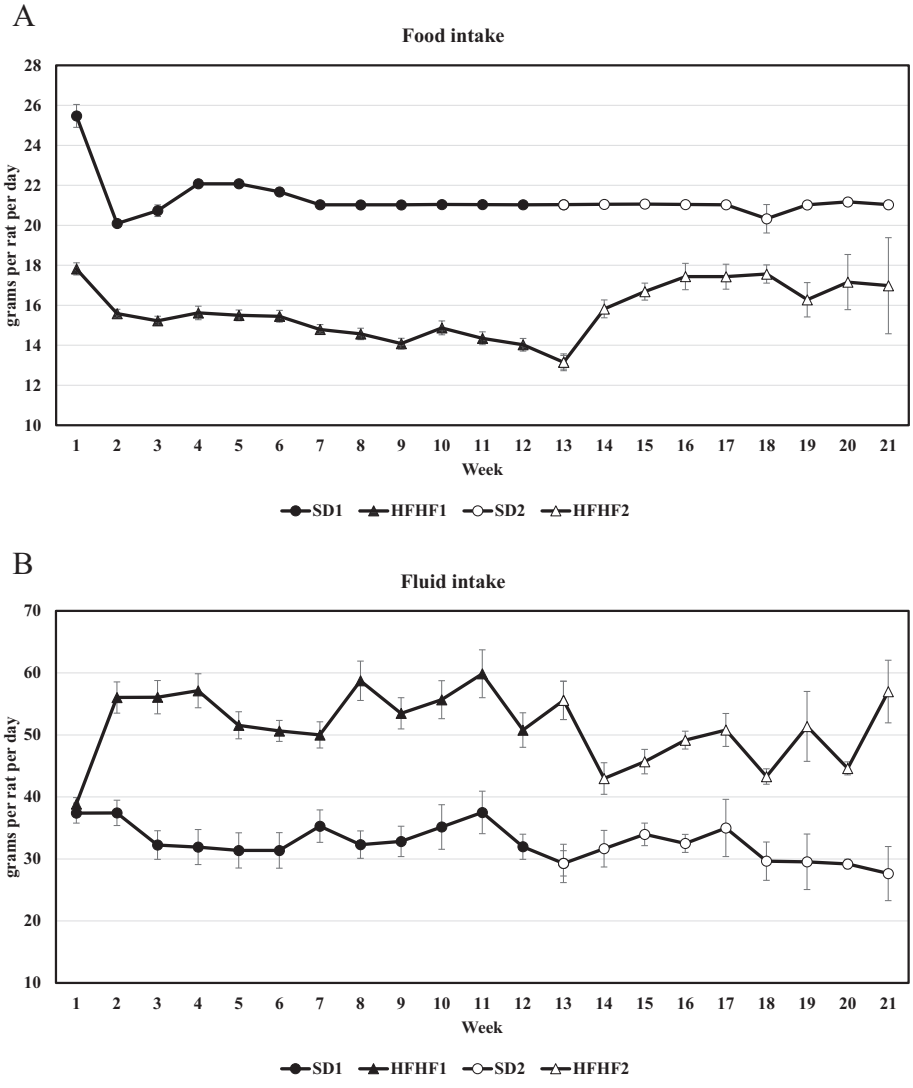

Fig. 1. Effect of DIO and length of experimental period on food (grams per rat per day, Fig. 1A), fluid (tap water or 20 % fructose solution, grams per rat per day, Fig. 1B) or caloric intake (kcal per rat per day, Fig. 1C), and bodyweight gain (grams, Fig. 1D) of Sprague-Dawley rats. To differentiate the results more clearly, only the most representative weeks of the experimental period are included in the graphs. SD1, standard diet for 13 weeks; HFHF1, high-fat high-fructose diet for 13 weeks; SD2 standard diet for 21 weeks; HFHF2, high fat-diet for 21 weeks. Points and bars represent the mean and standard error of the mean, respectively (n = 8).

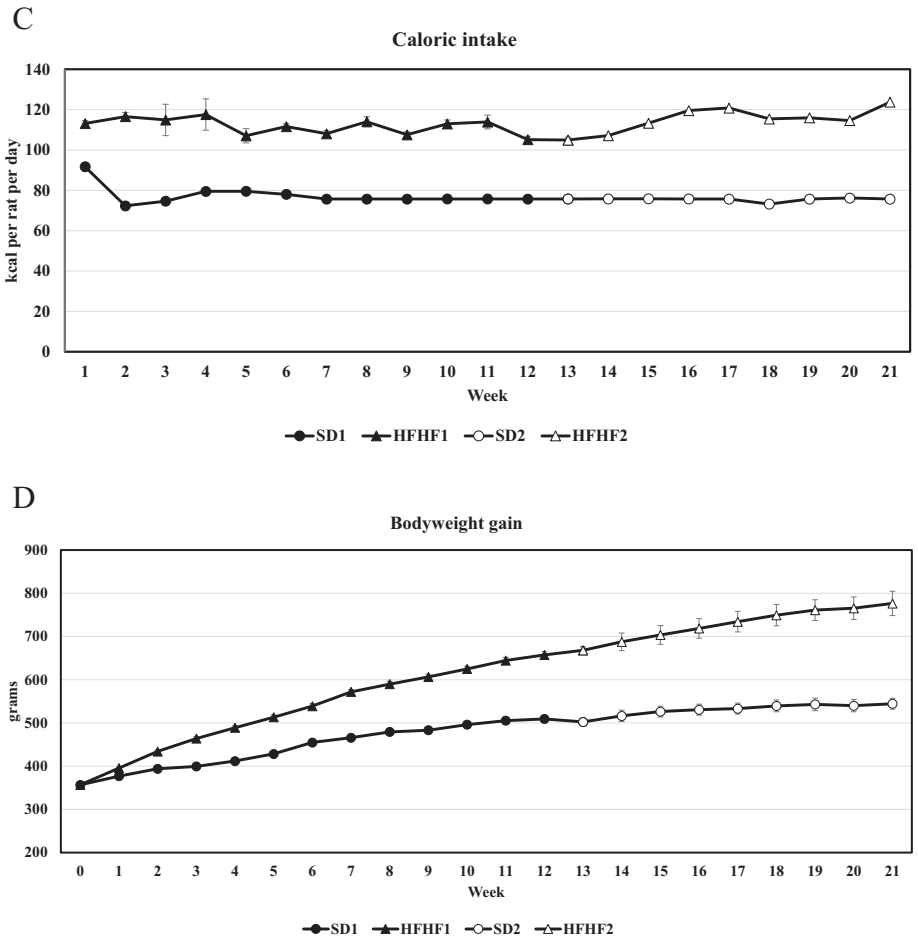

Fig. 1. (*continued*).

hepatic lobule in the form of columns that extended radially (Fig. 3C).

NAFLD scoring index (NAS), points out to hepatic histological alterations that may be potentially reverted such as steatosis, lobular inflammation, and ballooning. Scores for rats fed the SD diet along the 13 or 21-week experimental period corresponded to a value of 2 (no NASH), whereas DIO during 13 or 21 weeks led to values of 3 and 4 (probable NASH), respectively (Supplementary Table S2).

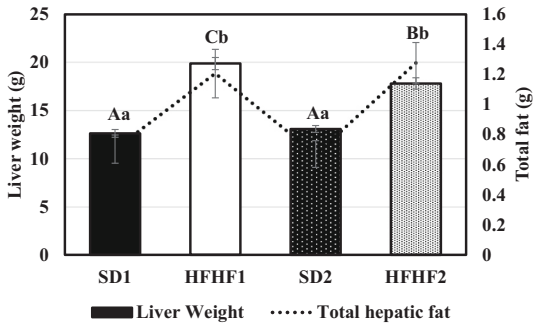

Fig. 2. Effect of dietary treatment and length of experimental period on liver and total hepatic fat weight (g). Columns or points and bars represent the mean and standard error of the mean, respectively (n = 8). Values within each treatment followed by different letters are significantly different (A–C, liver weight; a–b, total liver fat) $P < 0.05$. SD1, standard diet for 13 weeks; HFHF1, high-fat high-fructose diet for 13 weeks; SD2 standard diet for 21 weeks; HFHF2, high-fat high-fructose diet for 21 weeks. Liver weight, Diet effect: $P < 0.001$; Diet × Time: $P = 0.02$. Total fat, Diet effect: $P < 0.001$.

3.4. Fatty acid profile

The effect of dietary treatment and length of the experimental period on hepatic fatty acid profile and ratios is presented in Table 2. The highest proportion of hepatic fatty acids corresponded to saturated (palmitic and stearic acids), followed by mono- (palmitoleic, oleic, and octadecenoic acids) and poly-unsaturated fatty acids (linoleic, dihomo-γ-linolenic (DGLA), arachidonic and docosahexaenoic). Diet-induced obesity (DIO) had a significant effect on hepatic fatty acid profile, resulting in higher oleic and linoleic acid percentages, together with lower percentages of saturated acids (palmitic and stearic), palmitoleic, stearic, DGLA, and docosahexaenoic acids.

Elongase–desaturase ratios (docosahexaenoic/linolenic and arachidonic/linoleic) were significantly modified by diet administration, with lower ratios in the animals that consumed SD *vs* HFHF. Furthermore, stearoyl CoA desaturase activity was differentially affected by DIO, showing higher values for the oleic/stearic ratio and lower for the palmitoleic/palmitic ratio. The palmitoleic/palmitic ratio was also altered by the length of the experimental period, declining at week 21. Δ5-Desaturase activity (arachidonic/DGLA) was characterized by the opposite effects of DIO related to the length of experimental period (decrease at 13 weeks or increase at 21 weeks), thus resulting in a significant diet × time interaction.

3.5. Liver transcriptomic analysis

A complete hepatic transcriptomic profile (>32,000 genes, Fig. 4) was carried out in SD or HFHF-fed rats to study the influence of dietary treatment and length of experimental period on cell structure, glucose,

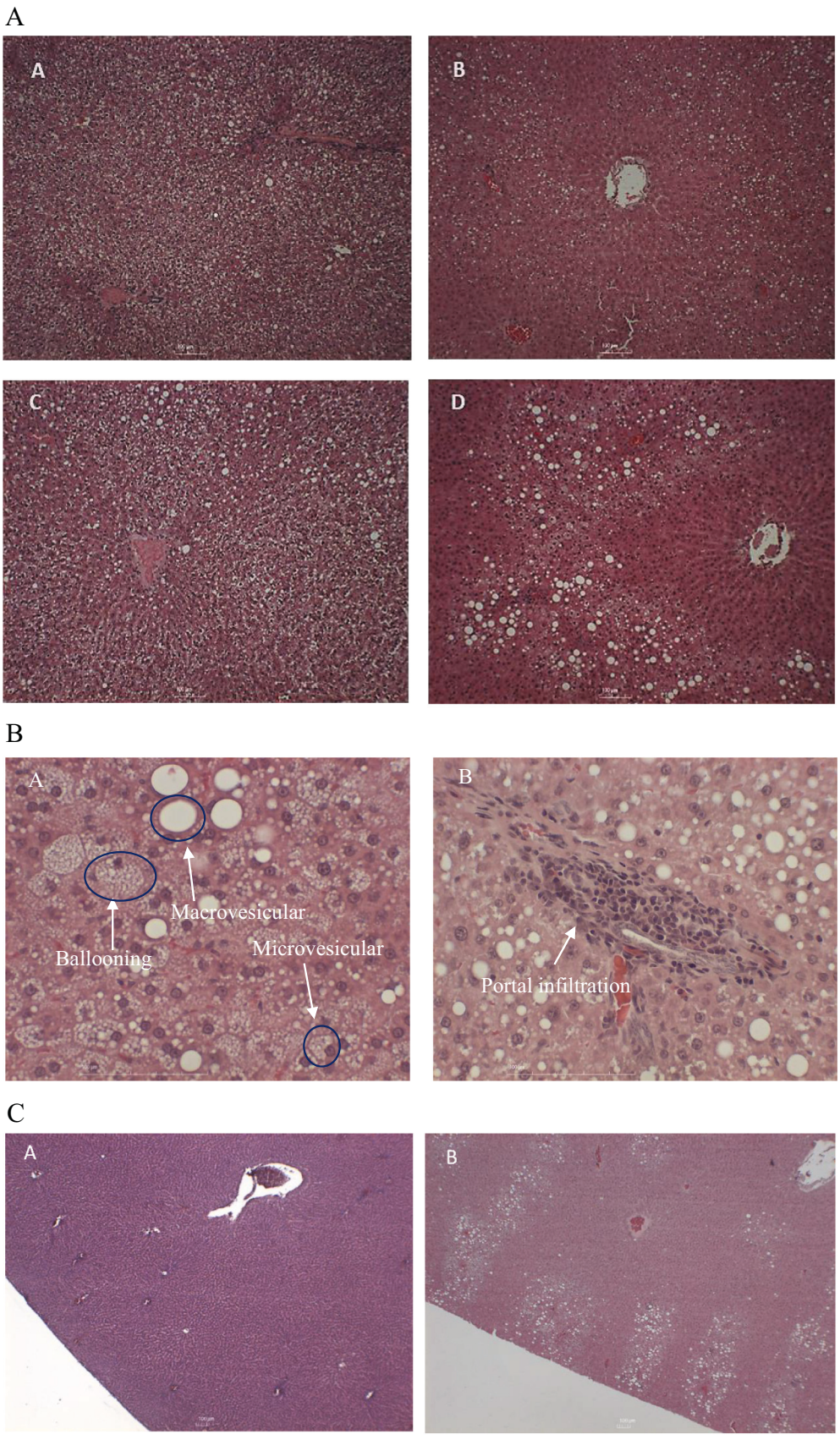

Fig. 3. Light microscopic images of liver preparations from rats fed SD or HFHF diets along 13 or 21 weeks of experimental period. Fig. 3A, effect of dietary induction of obesity and length of experimental period on liver histology (hematoxylin-eosin stain) of Sprague Dawley rats (50×). (A) SD1, (B) SD2, (C) HFHF1, (D) HFHF2. Photographs are representative of livers of 8 different rats for each experimental group. Fig. 3B, major alterations in hepatic histology caused by the dietary treatment and length of experimental period. A, steatosis, B, inflammation (hematoxylin-eosin stain, 200×). Photographs are representative of livers of 8 different rats for each experimental group. Fig. 3C, micrographs depicting the convex area of hepatic preparations from different experimental groups of Sprague-Dawley rats (hematoxylin-eosin stain, 20×). A, standard rodent chow (13 weeks), B, HFHF2. Photographs are representative of livers of 8 different rats for each experimental group. SD1, standard diet for 13 weeks; HFHF1, high-fat high-fructose diet for 13 weeks; SD2 standard diet for 21 weeks; HFHF2, high-fat high-fructose diet for 21 weeks.

Table 2
Influence of diet-induced obesity and length of experimental period on hepatic fatty acid profile (%) and fatty acid indices of rats.

	SD 13-weeks	HFHF 13-weeks	SD 21-weeks	HFHF 21-weeks	R^2	SEM	Diet effect	Time effect	Diet × Time effect
Palmitic (C16:0)	29.9 A	27.0 A	33.8 B	26.4 A	0.58	0.84	$P < 0.001$	$P = 0.096$	$P = 0.026$
Palmitoleic (C16:1)	5.92 B	4.37 AB	5.39 B	2.46 A	0.44	0.50	$P < 0.001$	$P = 0.038$	$P = 0.222$
Stearic (C18:0)	11.4 B	7.56 A	10.1 AB	9.41 AB	0.27	0.68	$P = 0.006$	$P = 0.71$	$P = 0.048$
Oleic (C18:1n9)	25.6 A	31.2 B	26.4 AB	29.3 AB	0.21	1.26	$P = 0.006$	$P = 0.713$	$P = 0.339$
Linoleic (C18:2n6)	9.56 AB	14.1 BC	8.61 A	17.4 C	0.55	1.10	$P < 0.001$	$P = 0.356$	$P = 0.098$
Dihomo-γ-linolenic (C20:3n6)	0.36 B	0.32 AB	0.36 B	0.21 A	0.36	0.03	$P = 0.004$	$P = 0.063$	$P = 0.086$
Arachidonic (C20:4n6)	10.5 A	7.84 A	9.55 A	9.73 A	0.13	0.91	$P = 0.242$	$P = 0.631$	$P = 0.18$
Docosahexaenoic (C22:6n3)	2.28 B	1.23 A	2.04 B	1.61 AB	0.32	0.18	$P = 0.001$	$P = 0.741$	$P = 0.137$
Octadecenoic (C18:1n7)	4.08 B	3.91 AB	3.16 AB	2.83 A	0.27	0.26	$P = 0.391$	$P = 0.002$	$P = 0.789$
Others	1.28 A	1.61 B	1.19 A	1.34 A	0.44	0.06	$P = 0.001$	$P = 0.01$	$P = 0.161$
SFA	41.4 B	35.6 A	44.8 C	36.0 A	0.75	0.76	$P < 0.001$	$P = 0.034$	$P = 0.101$
MUFA	35.6 A	39.6 A	35.0 A	34.7 A	0.07	1.62	$P = 0.309$	$P = 0.138$	$P = 0.239$
PUFA	23.0 AB	24.8 AB	20.2 A	29.3 B	0.29	1.63	$P = 0.006$	$P = 0.645$	$P = 0.058$
DC/LN	11.2 AB	5.65 A	16.1 B	5.20 A	0.53	1.42	$P < 0.001$	$P = 0.169$	$P = 0.103$
ARA/LE	1.13 B	0.62 B	1.22 B	0.61 A	0.53	0.09	$P < 0.001$	$P = 0.709$	$P = 0.599$
PE/PI	0.20 B	0.16 B	0.16 AB	0.09 A	0.39	0.02	$P = 0.006$	$P = 0.004$	$P = 0.403$
OLE/STE	2.61 A	4.65 A	2.75 A	3.75 A	0.16	0.52	$P = 0.014$	$P = 0.516$	$P = 0.375$
ARA/EI	34.9 AB	27.0 A	26.8 A	49.8 B	0.44	3.53	$P = 0.068$	$P = 0.077$	$P = 0.001$

SFA, saturated fatty acids; MUFA, monounsaturated fatty acids; PUFA, polyunsaturated fatty acids; DC/LN, docosahexaenoic/linolenic acid (desaturase–elongase); ARA/LE, arachidonic/linoleic acid (desaturase–elongase); PE/PI, palmitoleic/palmitic acid (Scd-1 activity); OLE/STE, oleic/stearic acid (Scd-1 activity); ARA/EI, arachidonic/DGLA acid (5-desaturase). Results are means of 8 rats. R^2, coefficient of determination, SEM, pooled standard error of the mean. A-C Means within the same row with different letters differ significantly ($P < 0.05$). SD, standard diet, HFHF, high-fat high-fructose diet.

and lipid metabolism as well as antioxidant and detoxifying enzyme activity. As expected, profound changes in hepatic gene expression were induced by these two factors. When comparing the DIO and lean rats on week 13 of the experimental period, a total of 4506 hepatic transcripts were differentially regulated according to the two-filter criteria (FC > 1.3 or <−1.3, $P < 0.05$). Of those, 645 transcripts were upregulated and 3861 downregulated in the HFHF1 *vs* SD1 group. Similar comparisons were made among the former groups and those in which the experimental period lasted for 21 weeks: SD2 *vs* SD1 (948 upregulated, 1551 downregulated), HFHF2 *vs* HFHF1 (3505 upregulated, 1364 downregulated), and HFHF2 *vs* SD2 (1222 upregulated, 1781 downregulated). Among those hepatic transcripts differentially regulated depending on the consumption of HFHF diet or length of experimental period, 32 were selected based on their physiological action and filtered into three categories: cell structure, glucose/lipid metabolism, and antioxidant & detoxifying capacity (Table 1).

3.6. Hepatic mRNA expression

To confirm the results of the hepatic transcriptome analysis, RT-qPCR expression analysis was carried out in the genes selected. The effects of dietary treatment and length of experimental period on the hepatic expression of transcripts involved in cell structure, lipid metabolism, and antioxidant & detoxifying activity are presented in Tables 3A–3D. The expression of genes grouped in the category of cell structure was differentially affected by the dietary treatment with an HFHF diet that resulted in a significant induction of *Col26a1*, *Psmb9*, *Gadd45a*, and *Slc2a2* compared to the SD diet on week 13 (Table 3A), whereas *Cdkn1a*, *Myc*, *Abcg5*, and *Slc34a2* were significantly down-regulated. On the other hand, HFHF treatment caused a significant increase in expression of *Cdkn1a*, *Gdf15*, *Myc*, and *Slc34a2 vs* SD on week 21, whereas it significantly decreased that of *Slc2a2*. Length of experimental period also exhibited a significant effect on gene expression, causing a general decrease in expression of most of the transcripts studied with the exception of *Mmp15* in both SD and HFHF groups or *CdKn1a* and *Myc* only in HFHF treatment.

Regarding the expression of lipogenic genes (Table 3B), mid-term DIO caused a marked up-regulation of transcription factor *Srebf1* and transcripts *Hmgcr*, *Pnpla3*, *Fasn*, *Scd1*, and *Fabp5* associated to cholesterol synthesis, hepatic fat accumulation, lipid and fatty acid synthesis or lipid transport on week 13. In contrast, most of the former transcripts and those related to cholesterol metabolism were down-regulated by HFHF consumption on week 21, which showed instead a significant up-regulation of transcription factor *Pparg* and transcript *Gck* associated to glucose metabolism. Aging showed a differential action on either SD or HFHF groups. In the former, it resulted in down-regulation of transcription factors and marked up-regulation of genes associated to cholesterol metabolism, hepatic fat accumulation, lipid and fatty acid synthesis. In contrast, aging down-regulated most transcripts related to lipogenesis in the HFHF intervention with the exception of *Gck* that was up-regulated.

Gene expression of lipolytic transcripts *Cpt1a,* and *Cyp7a1* was significantly down-regulated by the dietary treatment at both mid- and long-term obesity induction (Table 3C), while *Crot* was not affected at 13 weeks and exhibited a significant up-regulation on week 21. No major effect was found for the transcription factor *Ppara*. Length of experimental period also affected gene expression in both control and obesogenic groups; in the former, a significant up-regulation of the transcription factor *Ppara* was observed whereas the opposite was true for *Crot*, *Cpt1a,* and *Cyp7a1* expression. Similar effects were observed in the obesogenic groups.

Results of antioxidant and detoxifying enzyme gene expression are marked by two different trends. First, a significant interaction between DIO and the length of experimental period characterized the expression of *Akr7a3* or *Sod1* that were significantly up-regulated by DIO on week 13, but significantly down-regulated by this same treatment on week 21 (Table 3D). Second, a constant effect of the dietary treatment was observed along the experimental period for *Gpx* (up-regulated) or *Ucp2* (down-regulated) expression. A clear aging effect in both SD and HFHF groups was only observed for the expression of the transcription factor *Nfe212* and for *Sod1* which were lower on week 21 *vs* 13. The expression of *Akr7a3* and *Nqo1* transcripts was not affected by length of experimental period on the control SD groups, but exhibited a significant down-regulation in the obese animals.

3.7. Hepatic antioxidant and detoxifying enzyme activities

The effects of dietary treatment and length of experimental period on hepatic antioxidant and detoxifying enzyme activities are shown in Table 4. DIO had a significant effect during the entire experimental period in CAT, Mn-SOD, GST, and QR activities. CAT and GST were increased by the HFHF treatment whereas the opposite action was

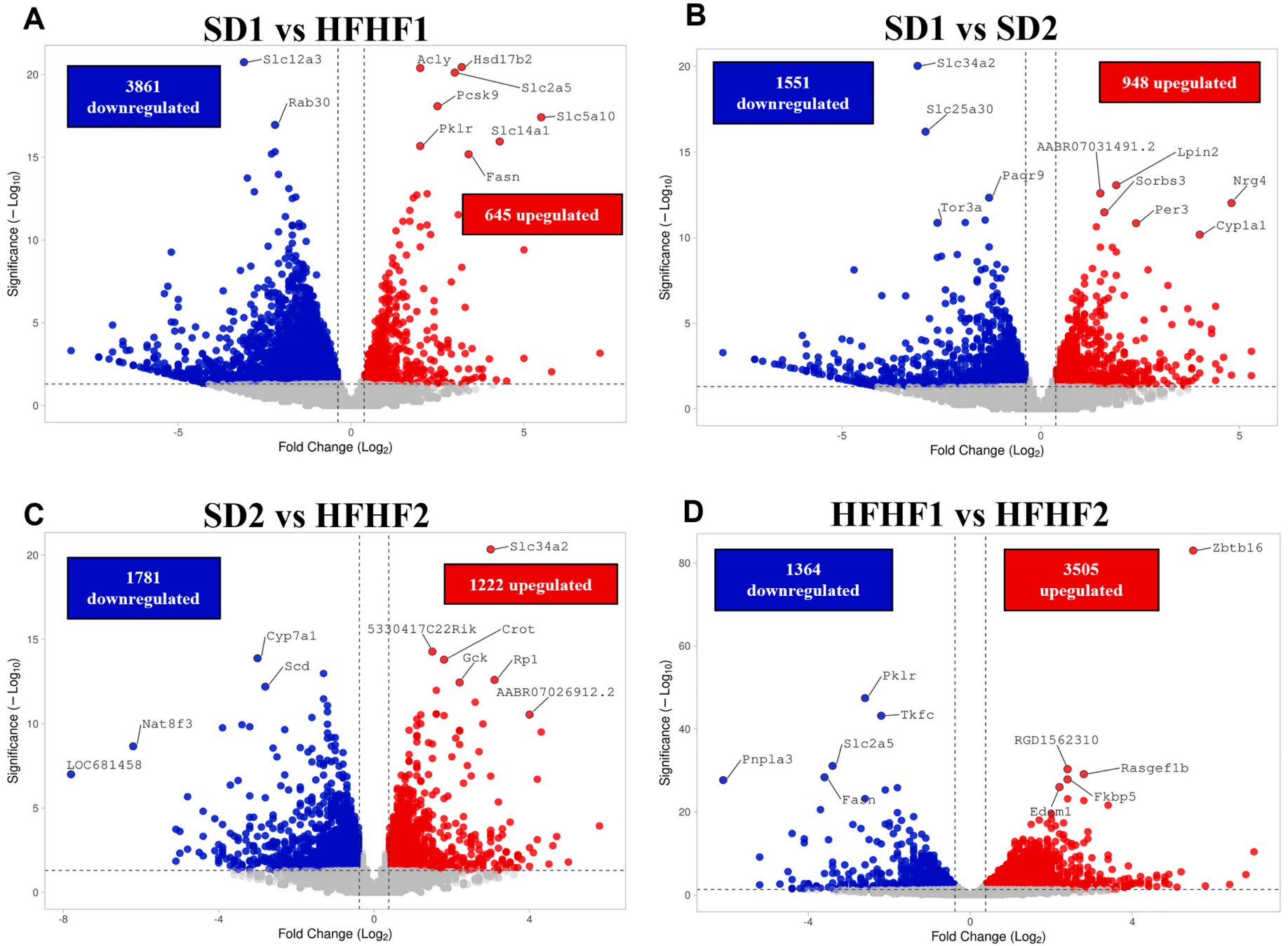

Fig. 4. Volcano plot showing the differentially regulated hepatic transcripts between the experimental groups (n = 6): (a) SD1 *vs* HFHF1, (b) SD1 *vs* SD2, (c) SD2 *vs* HFHF2, and (d) HFHF1 *vs* HFHF2. The double filtering criteria are indicated by horizontal (*P*-value <0.05) and vertical (fold change (FC): >log2 (1.3) or <log2 (−1.3)) dashed lines. Transcripts in the upper left and the upper right corner represent the downregulated and the upregulated transcripts, respectively.

Table 3A
Influence of dietary treatment and length of experimental period on hepatic expression of transcripts related to cell structure.

Function	Gene	SD1 *vs* HFHF1			SD1 *vs* SD2			SD2 *vs* HFHF2			HFHF1 *vs* HFHF2		
		SD1	HFHF1	*P-value*	SD1	SD2	*P-value*	SD2	HFHF2	*P-value*	HFHF1	HFHF2	*P-value*
Anatomic cell structure	*Mmp15*	1.00 ± 0.09	0.90 ± 0.09	0.46	1.00 ± 0.09	1.51 ± 0.21	0.041	1.00 ± 0.14	1.05 ± 0.08	0.743	1.00 ± 0.10	1.76 ± 0.13	<0.001
	Psmb9	1.00 ± 0.11	1.63 ± 0.15	0.005	1.00 ± 0.11	0.81 ± 0.10	0.215	1.00 ± 0.13	0.99 ± 0.11	0.971	1.00 ± 0.09	0.49 ± 0.05	<0.001
Cell adhesion	*Col26a1*	1.00 ± 0.09	11.2 ± 3.88	0.065	1.00 ± 0.09	1.37 ± 0.26	0.302	1.00 ± 0.19	3.44 ± 1.64	0.163	1.00 ± 0.35	0.42 ± 0.20	0.167
Cell damage	*Cdkn1a*	1.00 ± 0.14	0.58 ± 0.14	0.051	1.00 ± 0.14	0.57 ± 0.10	0.023	1.00 ± 0.18	2.07 ± 0.27	0.005	1.00 ± 0.24	2.01 ± 0.26	0.013
	Gadd45a	1.00 ± 0.18	1.54 ± 0.13	0.03	1.00 ± 0.18	0.62 ± 0.05	0.06	1.00 ± 0.08	0.86 ± 0.12	0.36	1.00 ± 0.09	0.35 ± 0.05	<0.001
Cell proliferation	*Gdf15*	1.00 ± 0.16	1.04 ± 0.14	0.859	1.00 ± 0.16	0.44 ± 0.07	0.006	1.00 ± 0.15	1.65 ± 0.21	0.026	1.00 ± 0.13	0.69 ± 0.09	0.073
	Myc	1.00 ± 0.18	0.38 ± 0.04	0.004	1.00 ± 0.18	0.39 ± 0.03	0.004	1.00 ± 0.09	2.14 ± 0.18	<0.001	1.00 ± 0.11	2.15 ± 0.19	<0.001
Solute transport	*Abcg5*	1.00 ± 0.20	0.27 ± 0.06	0.003	1.00 ± 0.20	0.27 ± 0.07	0.004	1.00 ± 0.27	1.58 ± 0.27	0.15	1.00 ± 0.22	1.61 ± 0.28	0.106
	Slc2a2	1.00 ± 0.11	1.48 ± 0.14	0.02	1.00 ± 0.11	1.15 ± 0.09	0.319	1.00 ± 0.08	0.61 ± 0.07	0.002	1.00 ± 0.10	0.47 ± 0.05	<0.001
	Slc34a2	1.00 ± 0.10	0.65 ± 0.13	0.049	1.00 ± 0.10	0.21 ± 0.03	<0.001	1.00 ± 0.13	4.02 ± 0.46	<0.001	1.00 ± 0.20	1.28 ± 0.15	0.263

qRT-PCR analysis of *Mmp15*, Matrix metalloproteinase-15; *Psmb9*, Proteasome subunit beta type-9; *Col26a1*, Collagen alpha-1(XXVI) chain; *Cdkn1a*, Cyclin-dependent kinase inhibitor 1; *Gadd45a*, Growth arrest and DNA damage-inducible protein alpha; *Gdf15,* Growth/differentiation factor 15; *Myc*, Myc proto-oncogene protein; *Abcg5,* ATP-binding cassette sub-family G member 5; *Slc2a2*, Solute carrier family 2, facilitated glucose transporter member 2; *Slc34a2*, Sodium-dependent phosphate transport protein 2B. Results are means ± SEM fold changes of 8 rats. SD1, standard diet for 13 weeks; HFHF1, high-fat high-fructose diet for 13 weeks; SD2 standard diet for 21 weeks; HFHF2, high-fat high-fructose diet for 21 weeks.

Table 3B
Influence of dietary treatment and length of experimental period on hepatic expression of transcripts related to glucose and lipid metabolism.

Function	Gene	SD1 *vs* HFHF1			SD1 *vs* SD2			SD2 *vs* HFHF2			HFHF1 *vs* HFHF2		
		SD1	HFHF1	*P-value*	SD1	SD2	*P-value*	SD2	HFHF2	*P-value*	HFHF1	HFHF2	*P-value*
Transcription factor	*Srebf1*	1.00 ± 0.25	3.13 ± 0.47	0.001	1.00 ± 0.25	0.53 ± 0.11	0.113	1.00 ± 0.20	1.08 ± 0.09	0.735	1.00 ± 0.15	0.18 ± 0.02	<0.001
	Pparg	1.00 ± 0.07	1.21 ± 0.14	0.216	1.00 ± 0.07	0.39 ± 0.05	<0.001	1.00 ± 0.12	1.92 ± 0.28	0.01	1.00 ± 0.12	0.62 ± 0.09	0.021
Cholesterol metabolism	*Cyp1a1*	1.00 ± 0.16	1.30 ± 0.35	0.449	1.00 ± 0.16	6.83 ± 2.72	0.05	1.00 ± 0.40	0.19 ± 0.03	0.061	1.00 ± 0.27	0.98 ± 0.14	0.959
	Cyp1a2	1.00 ± 0.15	0.45 ± 0.05	0.003	1.00 ± 0.15	1.58 ± 0.27	0.085	1.00 ± 0.17	0.57 ± 0.07	0.037	1.00 ± 0.12	2.01 ± 0.24	0.002
	Hmgcr	1.00 ± 0.21	1.55 ± 0.21	0.087	1.00 ± 0.21	1.52 ± 0.11	0.049	1.00 ± 0.07	0.71 ± 0.16	0.128	1.00 ± 0.13	0.70 ± 0.16	0.17
Glucose metabolism	*Gck*	1.00 ± 0.23	0.55 ± 0.09	0.086	1.00 ± 0.23	0.67 ± 0.08	0.203	1.00 ± 0.12	3.55 ± 0.30	<0.001	1.00 ± 0.16	4.39 ± 0.37	<0.001
Hepatic fat accumulation	*Pnpla3*	1.00 ± 0.42	13.0 ± 4.60	0.021	1.00 ± 0.42	3.82 ± 1.09	0.03	1.00 ± 0.28	0.14 ± 0.04	0.01	1.00 ± 0.35	0.04 ± 0.01	0.017
Lipid and fatty acid synthesis	*Agpat3*	1.00 ± 0.11	0.91 ± 0.07	0.507	1.00 ± 0.11	0.64 ± 0.11	0.039	1.00 ± 0.17	1.51 ± 0.21	0.083	1.00 ± 0.08	1.07 ± 0.15	0.702
	Fasn	1.00 ± 0.12	6.72 ± 0.64	<0.001	1.00 ± 0.12	3.88 ± 0.50	<0.001	1.00 ± 0.13	0.25 ± 0.04	<0.001	1.00 ± 0.09	0.14 ± 0.02	<0.001
	Scd1	1.00 ± 0.42	5.42 ± 1.03	0.001	1.00 ± 0.42	3.89 ± 0.42	<0.001	1.00 ± 0.11	0.17 ± 0.03	<0.001	1.00 ± 0.19	0.12 ± 0.02	<0.001
Lipid transport	*Fabp5*	1.00 ± 0.15	2.91 ± 0.65	0.012	1.00 ± 0.15	1.40 ± 0.31	0.268	1.00 ± 0.22	0.16 ± 0.04	0.002	1.00 ± 0.22	0.08 ± 0.02	0.001

qRT-PCR analysis of *Srebf1*, Sterol regulatory element binding transcription factor 1; *Pparg*, Peroxisome proliferator-activated receptor gamma; *Cyp1a1*, Cytochrome P450 1A1; *Cyp1a2*, Cholesterol 25-hydroxylase; *Hmgcr*, 3-hydroxy-3-methylglutaryl-coenzyme A reductase; *Gck*, Hexokinase-4; *Pnpla3,* Patatin-like phospholipase domain-containing protein 3; *Agpat3*, 1-acyl-sn-glycerol-3-phosphate acyltransferase gamma; *Fasn*, fatty acid synthase; *Scd1*, stearoyl-CoAdesaturase-1 and *Fabp5*, Fatty acid-binding protein 5. Results are means ± SEM fold changes of 8 rats. SD1, standard diet for 13 weeks; HFHF1, high-fat high-fructose diet for 13 weeks; SD2 standard diet for 21 weeks; HFHF2, high-fat high-fructose diet for 21 weeks.

observed for Mn-SOD and QR activities. A significant time effect was observed in Cu/Zn-SOD, Mn-SOD, and GPX activities related to their decreased values at 21 *vs* 13 weeks. Regarding diet × time interactions, they were derived either from a differential action (increase or decrease of the enzymatic activity) of the dietary treatment at 13 or 21 weeks, such is the case with Cu/Zn SOD and GPX, or from the greater strength of the dietary treatment in a specific stage, such as with CAT and QR activities. Pearson correlation analysis between antioxidant enzyme gene or transcript expression and enzyme activity is presented in Table 5. Positive correlations were found between gene expression and enzyme activity for *Sod1* and *Nqo1*, whereas no correlation was found between glutathione peroxidase expression and activity. Results of transcriptome analysis denoted a high positive correlation between GST activity and the expression of several *Gst* functional genes, among which *Gstm1* was of special relevance. A weaker correlation was found between Mn-SOD activity and *Sod2* expression, whereas no correlation was found between

Table 3C
Influence of dietary treatment and length of experimental period on hepatic expression of transcripts related to lipolytic action.

Function	Gene	SD1 *vs* HFHF1			SD1 *vs* SD2			SD2 *vs* HFHF2			HFHF1 *vs* HFHF2		
		SD1	HFHF1	*P-value*	SD1	SD2	*P-value*	SD2	HFHF2	*P-value*	HFHF1	HFHF2	*P-value*
Transcription factor	*Ppara*	1.00 ± 0.11	1.19 ± 0.53	0.733	1.00 ± 0.11	1.98 ± 0.19	<0.001	1.00 ± 0.09	0.91 ± 0.08	0.487	1.00 ± 0.45	1.52 ± 0.14	0.287
Fatty acid β-oxidation	*Cpt1a*	1.00 ± 0.08	0.67 ± 0.05	0.004	1.00 ± 0.08	0.57 ± 0.04	<0.001	1.00 ± 0.07	0.70 ± 0.09	0.02	1.00 ± 0.08	0.59 ± 0.08	0.003
	Crot	1.00 ± 0.10	1.19 ± 0.15	0.324	1.00 ± 0.10	0.58 ± 0.09	0.009	1.00 ± 0.15	2.96 ± 0.47	0.001	1.00 ± 0.13	1.45 ± 0.23	0.11
Cholesterol to bile acids	*Cyp7a1*	1.00 ± 0.34	0.30 ± 0.03	0.059	1.00 ± 0.34	0.36 ± 0.07	0.086	1.00 ± 0.19	0.20 ± 0.03	0.001	1.00 ± 0.11	0.24 ± 0.04	<0.001

qRT-PCR analysis of *Ppara*, Peroxisome proliferator activated receptor alpha, *Cpt1a*, Carnitine palmitoyl transferase 1A; *Crot*, Peroxisomal carnitine O-octanoyl-transferase and *Cyp7a1*, Cholesterol 7 alpha-hydroxylase. Results are means ± SEM fold changes of 8 rats. SD1, standard diet for 13 weeks; HFHF1, high-fat high-fructose diet for 13 weeks; SD2 standard diet for 21 weeks; HFHF2, high-fat high-fructose diet for 21 weeks.

Table 3D
Influence of dietary treatment and length of experimental period on hepatic expression of transcripts related to antioxidant or detoxifying activity.

Function	Gene	SD1 *vs* HFHF1			SD1 *vs* SD2			SD2 *vs* HFHF2			HFHF1 *vs* HFHF2		
		SD1	HFHF1	*P-value*	SD1	SD2	*P-value*	SD2	HFHF2	*P-value*	HFHF1	HFHF2	*P-value*
Transcription factor	*Nfe2l2*	1.00 ± 0.09	1.02 ± 0.15	0.925	1.00 ± 0.09	0.61 ± 0.06	0.003	1.00 ± 0.09	1.28 ± 0.09	0.041	1.00 ± 0.15	0.78 ± 0.05	0.175
Antioxidant activity	*GPX1*	1.00 ± 0.11	1.77 ± 0.20	0.004	1.00 ± 0.11	1.11 ± 0.15	0.555	1.00 ± 0.13	1.53 ± 0.17	0.026	1.00 ± 0.11	0.96 ± 0.10	0.792
	SOD1	1.00 ± 0.20	1.65 ± 0.12	0.016	1.00 ± 0.20	0.79 ± 0.13	0.398	1.00 ± 0.16	0.75 ± 0.13	0.257	1.00 ± 0.07	0.36 ± 0.06	<0.001
	Ucp2	1.00 ± 0.11	0.76 ± 0.09	0.107	1.00 ± 0.11	1.17 ± 0.09	0.243	1.00 ± 0.08	0.70 ± 0.03	0.004	1.00 ± 0.11	1.09 ± 0.05	0.494
Detoxifying activity	*Akr7a3*	1.00 ± 0.12	2.65 ± 0.22	<0.001	1.00 ± 0.12	1.48 ± 0.26	0.118	1.00 ± 0.18	0.47 ± 0.05	0.013	1.00 ± 0.08	0.27 ± 0.03	<0.001
	Nqo1	1.00 ± 0.13	1.08 ± 0.20	0.729	1.00 ± 0.13	1.26 ± 0.17	0.239	1.00 ± 0.13	0.45 ± 0.10	0.005	1.00 ± 0.19	0.52 ± 0.11	0.045

qRT-PCR analysis of *Nfe2l2*, nuclear factor erythroid 2 like2; *GPX1,* Glutathione peroxidase 1; *SOD1*, Superoxide dismutase [Cu-Zn]; *Ucp2*, Mitochondrial uncoupling protein 2; *Akr7a3*, Aflatoxin B1 aldehyde reductase member 3 and *Nqo1*, NAD(*P*)H: quinone oxidoreductase 1 Results are means ± SEM fold changes of 8 rats. SD1, standard diet for 13 weeks; HFHF1, high-fat high-fructose diet for 13 weeks; SD2 standard diet for 21 weeks; HFHF2, high-fat high-fructose diet for 21 weeks.

Table 4
Hepatic activity of antioxidant and detoxifying enzymes.

Function	Enzyme	SD 13-weeks	HFHF 13-weeks	SD 21-weeks	HFHF 21-weeks	R^2	SEM	Diet effect	Time effect	Diet × Time effect
Antioxidant activity	CAT	7.8 A	19.3 C	11.8 B	14.7 B	0.742	0.873	$P < 0.001$	$P = 0.770$	$P < 0.001$
	GPx	14.4 B	14.4 B	13.8 B	9.5 A	0.357	0.914	$P = 0.026$	$P = 0.005$	$P = 0.027$
	Mn-SOD	30.5 AB	48.0 C	37.5 B	28.1 A	0.546	2.435	$P = 0.109$	$P = 0.013$	$P < 0.001$
	Cu/Zn-SOD	1433.3 B	1365.6 B	1175.3 AB	898.6 A	0.355	86.0	$P = 0.014$	$P = 0.001$	$P = 0.558$
Detoxifying activity	GST	708.3 A	958.4 B	720.4 A	813.4 AB	0.271	52.479	$P = 0.003$	$P = 0.216$	$P = 0.146$
	QR	198.4 B	182.6 B	217.2 B	106.4 A	0.351	18.929	$P = 0.002$	$P = 0.141$	$P = 0.018$

Results are means of 8 rats. R^2, coefficient of determination, SEM, pooled standard error of the mean. CAT (UAE/min·mg prot), catalase; SOD (UAE/min·mg prot), superoxide dismutase; GPx (nmol NADPH/min·mg prot), glutathione peroxidase; GST (UA/mg prot), glutathione transferase; QR (UA/mg prot), NADH:Quinone Reductase. A-C Means within the same row with different letters differ significantly ($P < 0.05$). SD, standard diet, HFHF, high-fat high-fructose diet.

Table 5
Pearson correlation between gene or transcript expression and enzyme activity.

	Pearson coefficient	*P-value*
Mn-SOD (enzymatic activity-transcript expression)	0.448	0.028
Cu/Zn-SOD (enzymatic activity-gene expression)	0.500	0.004
GST (enzymatic activity-transcript expression)	0.557	0.005
QR (enzymatic activity-gene expression)	0.575	0.001

SOD, superoxide dismutase; GST, glutathione transferase; QR: NADH:Quinone Reductase.

the gene expression and activity of catalase.

4. Discussion

This study aimed to define and standardize the development of a diet-induced obesity model and to study the effect of mid-term (13 weeks) and long-term high-fat high-fructose diet consumption (21 weeks) on cell structure components, glucose and lipid metabolism, or hepatic antioxidant and detoxifying defense system. This aging process in obese rats was compared to the same process in lean rats. To achieve this objective, a high-fat high-fructose diet was consumed and food intake, bodyweight, liver fat content, fatty acid profile, gene expression of lipogenic, lipolytic and antioxidant enzymes, as well as antioxidant status, were assessed. The model tested has a high similarity to the

metabolic profile of the human disease: obesity, insulin resistance, and increased serum free fatty acids (FFA) and liver triglycerides (TG) content that are found beginning at 10 weeks after feeding an HF diet in mice and rats [6].

The consumption of the high fat/high fructose diet led to obesity establishment (the difference in body weight between standard and experimental diet-fed animals was equal to or >2 standard deviations) from the third week of experimental period. Thus, showing a greater efficiency compared to a previous obesity induction strategy of a HFD (60 % kcal) in which the former differences were attained after five weeks of experimental period [9], or to what has been reported by Woods et al. [38] after feeding rats with high-fat non-fructose diet during 12 weeks. In addition, body weight changes due to DIO were similar to genetic obesity models [39]. In line with these results, we found dramatic changes in body mass composition after DIO that include a general increase in the total fat mass. Lipids tend to accumulate within lipid droplets in adipose tissue but also in non-adipose tissues, such as the liver. The excess of this ectopic lipid deposition and the alteration of lipid droplets homeostasis may contribute to the pathogenesis of metabolic syndrome-related diseases [40]. Mid- and long-term feeding of a HFD is known to increase liver weight [41,42]. Here, the induction of obesity also led to fat accumulation in the liver at both 13 and 21 weeks, which was accompanied by TG accumulation in the liver and plasma (data not shown).

We also found clear signs of liver steatosis and histological alterations that characterize the development of NAFLD. The NASH grading score gave a NAS score value of 3–4 based on the semiquantitative evaluation of steatosis and hepatocellular ballooning. Another interesting finding refers to the evolution in the steatosis pattern from microvesicular to macrovesicular change as rats aged during the experimental period. This change was more evident in rats in HFHF *vs* SD groups and agrees with the results of Kristiansen et al. [43] who reported an increment in macrovesicular change concurring with more advanced stages of the experimental period. Therefore, a relationship exists between the observed histological alterations and the length of time during which rats consume the experimental diets. With larger consumption periods, changes in hepatic histology became more detrimental and more likely to progress to more advanced stages of the disease such as fibrosis, cirrhosis, or hepatocarcinoma. On the other hand, hepatocyte ballooning, a histological alteration that also increased with the aging of rats, is associated with increased hepatocyte size due to an alteration in the intermediate filaments of the cytoskeleton derived from the rupture of cytokeratins 8 and 18 [44]. The greater extent of histological damage observed with aging runs in parallel to the accumulation of a greater fat amount in the liver, thus pointing out to the cumulative damage caused by larger exposure of the animals to the potentially deleterious effects of a dietary imbalance with excessive energy intake in the form of fat and monosaccharides like fructose. Regarding the presence of localized macrovesicular steatosis in the convex zone of the selected hepatic lobe section and the organization in rows with a radial disposition of the foci of hepatocytes with larger fat droplets (Fig. 3C), several studies show that localized steatosis in the liver can be related to hepatic blood irrigation in what is known as vascular theory [45,46]. In addition to the normal flow of the liver obtained by the portal vein and the hepatic artery, there are other flows called aberrant flows by the pancreaticoduodenal veins, the veins of Sappey, or the left and right aberrant gastric veins, constituting what is called the third inflow [47]. Focal fat is associated with the third inflow and various hormones in the portal flow that causes altered levels of TG and fatty acids.

One may expect that the alteration of the intracellular environment may also affect mitochondria leading to either functional impairment or adaptation through mechanisms such as changes in gene expression, affecting their antioxidant capacity [48]. Oxidative stress is considered to be a crucial event in the development of diet-induced obesity complications in rats [49]. Many studies [41,49] have shown an inverse relation between ROS levels and antioxidant activity, thus decreasing the protective capacity of the liver. In contrast, other studies, including our results at 13 weeks, showed that mid-term consumption of a HFD increased the activity of antioxidant and detoxifying enzymes, CAT, Mn-SOD, and GST, probably in an attempt to counteract the increased obesity-related ROS production [50].

Concerning liver antioxidant status, it is worth mentioning the significant increase in expression of genes related to antioxidant or detoxifying activity, *Gpx1*, *Sod1*, and *Akr7a3* by week 13 of the experimental period, once obesity was established. *Akr7a3* is involved in the detoxification process, and regulated by *Nfe2l2* expression [51,52], although no increase in *Nfe2l2* expression was observed after the intake of HFHF diet as would be expected. Nevertheless, NRF2 activity is known to be increased after its nuclear translocation, without the need for an increase in its gene expression [53].

Another important factor was consumption time since an obesity induction period of 13 weeks with this high-fat high-fructose does not seem to be long enough to observe an imbalance in the oxidative status. A longer obesity induction period of 21 weeks caused the expected effects, decreasing the activity of all hepatic antioxidant enzymes measured. In addition, a decrease in the expression of *Akr7a3*, *Nqo1,* and *Sod1* was observed after the long-term high-fat high-fructose diet administration, indicating an inefficient defense system against ROS. These findings point out again to aging during the experimental period related to a cumulative damage caused by exposure to the obesity induction interventions during longer time periods. In contrast, the enzymatic activity after the intake of a standard diet was unaltered by time (except for an increase in catalase activity) while *Ucp2*, *Akr7a3*, and *Nqo1*gene expression tended to increase (not significantly). Thus, an obesogenic diet when associated to aging process was a more crucial factor than only aging to affect antioxidant activity under the experimental conditions of the present study. Furthermore, a relevant finding concerning the antioxidant status of the liver was the highly significant correlation between changes in gene expression and antioxidant activity of Cu/Zn-SOD, Mn-SOD, QR, and GST. This result reflects a high dependence of enzymatic activity on the expression of the corresponding genes.

High fat and fructose intake led to hepatic fat accumulation and also modified the fatty acid profile compared to the animals fed a standard diet. A significant decrease in saturated fatty acids was observed while polyunsaturated fatty acid levels increased. These changes were maintained but not exacerbated by time. Importantly, replacing saturated fat with polyunsaturated fat makes the liver more susceptible to attack by ROS. As it has been reported in other studies, the mid- and long-term intake of a HFD based on lard mostly increases the levels of oleic (C18:1n9) and linoleic acid (C18:2n6), whereas it decreases docosahexaenoic acid (C22:6n3) levels [54,55]. The increase in oleic acid and decrease in stearic acid found in our study may be related to the higher oleic acid intake provided by the HFHF diet and/or indicate the activation of Δ-9 desaturase, which performs the conversion of C18:0 into C18:1n9 [55].

Oleic acid levels, PE/PI, and OLE/STE ratios are related to Stearoyl-CoA desaturase-1 (SCD1) activity and the ratios are often used as a surrogate measure for its activity. The consumption of a HFD for 13 weeks is related to an increase in *Scd1* gene expression and oleic acid level [56]. The trend of OLE/STE ratio was related to *Scd1* gene expression on week 13, but not PE/PI ratio. On the other hand, *Scd1* expression was modulated by diet × time interaction showing that aging in obese rats leads to reduced *Scd1* expression that was previously overexpressed by the mid-term development of obesity. Therefore, depending on the time chosen the level of gene expression can differ dramatically in *Scd1* and other lipogenic transcripts.

The combination of high fat and fructose intake plays an important role in the expression of different genes regulated by transcription factors such as SREBP-1, PPARA, and PPARG. In the liver, *de novo* lipogenesis is regulated by sterol regulatory element-binding protein-1 (SREBP-1) encoded by *Srebf1* and induced by insulin at multiple levels.

In contrast, it plays a minor role in adipocyte lipogenesis [57] which, in turn, is strongly influenced by *Pparg* [58]. Our results showed a clear increase in the gene expression of *Srebf1* accompanied by an increase in *Fasn*, *Scd1,* and *Hmgcr* expression after the intake of an HFHF diet for 13 weeks. In this regard, Flamment et al. [59] observed an increased *Srebf1* expression derived from HFD consumption along their final point of 8 weeks. Furthermore, the increase in hepatic fat accumulation could be also explained by a higher *Pnpla3* expression on week 13, which is highly related to NAFLD development [60]. Retinyl ester hydrolysis through *Pnpla3* expression and cholesterol homeostasis control through *Hmgcr* expression is also upregulated by *Srebf1* [61]. All this may indicate that the accumulation of fat in the liver at mid-term may be largely due to a rising of *de novo* lipogenesis. Fat accumulation also could be due to a higher flux of FFA to the liver due to upregulated expression of *Fabp5*. This upregulation matches that of other lipogenic transcripts (*Fasn*, *Hmgcr*, *Scd1*, *Pnpla3*) which exhibit a mid-term increase and a long-term decrease related to HFHF diet consumption.

The expression of the peroxisome proliferator-activated receptor gamma (*Pparg*), a master regulator of adipogenesis [57–59], was increased by the obesogenic dietary pattern at mid- or long-term consumption, although it should be emphasized that aging-associated obesity development led to a higher increase in the long run (1.21 *vs* 1.92-fold increase at 13 weeks *vs* 21 weeks). Lee *et al* [62] have described that *Pparg* expression levels positively correlate with fat accumulation induced by pathological conditions such as obesity and diabetes. The same pattern is observed in *Agpat3*, encoding an acyl transferase responsible for the conversion of lysophosphatidic acid to phosphatidic acid during *de novo* synthesis of phospholipids [63].

Another important mechanism of lipid metabolism control that takes place in hepatocytes is the β-oxidation of fatty acids in mitochondria where peroxisome proliferator-activated receptor alpha *(Ppara*) is a major transcriptional activator [56]. Under high lipogenic gene expression and reduced transcription of specific lipolytic genes (*Cpt1a* and *Cyp7a1*), the hepatic FFA would be incorporated into the hepatocytes instead of being oxidized [49,56]. In the long-term, the main mechanism of fat accumulation is the reduced fatty acid catabolism by oxidation in mitochondria (reduced expression of *Ppara*, *Cpt1a* and *Cyp7a1*), while in the mid-term is *de novo* lipogenesis.

Other genes involved in lipid metabolism and the development of obesity or NAFLD have been studied. Cyp family is the main group of enzymes involved in drug metabolism, but they are also related to cholesterol and lipid metabolism. These genes could be used as potential therapeutic candidates for NAFLD. In this sense, it is worth mentioning the increased expression of *Col26a1* gene, related to the development of non-alcoholic liver disease, on weeks 13 and 21. Besides, the oxidative stress conditions derived from the consumption of HFHF diet could in turn produce DNA damage and probably be associated with the increase of *Gadd45a* at 13 weeks or *Cdkn1a* at 21 weeks. Both genes code for proteins involved in cell damage. On the other hand, *Gdf15*, a gene associated to the stress response program of cells after cellular injury, and *Myc*, a proto-oncogene involved in numerous cancer processes, followed a similar pattern than *Cdkn1a* experiencing an increase at long-term induced by the HFHF diet intake.

5. Conclusions

The high fat and high fructose diet used defined a well-characterized obesity model that exhibited a marked imbalance in hepatic lipid metabolism and antioxidant status after a mid- (13 weeks) or long-term (21 weeks) experimental period, with cumulative damage due to the deleterious action of the high-fat/high-fructose diet in hepatic histology and antioxidant defense system. The main mechanisms of hepatic fat accumulation for mid- or long-term obesity induction were *de novo* lipogenesis or altered fatty acid catabolism by β-oxidation, respectively. Therefore, the choice of obesity-induction length is a key factor in the model of obesity studied and should be controlled in each specific experimental design.

5.1. Limitations

Although the SD diet is a very accurate control of the HFD, showing a similar chemical composition to the later diet and only differing in the amount of total fat and fructose, it causes some alterations in liver histology when compared to standard rat chow that contains a greater amount of plant-based protein and lower content of mono and disaccharides. In addition, gene expression and antioxidant activity data should be complemented with protein expression analysis to obtain a more extensive view of the influence of obesity on antioxidant status. Finally, since the results of the present study are obtained in a rat experimental model, they need to be confirmed in a human clinical study.

CRediT authorship contribution statement

Alejandro García-Beltrán: Investigation, Data curation, Formal analysis, Writing-Original Draft. **Rosario Martínez**: Conceptualization, Methodology, Investigation, Data curation, Formal analysis, Writing-Original Draft, Writing-Review & Editing. **Jesús M. Porres**: Conceptualization, Methodology, Investigation, Data curation, Writing-Original Draft, Writing-Review & Editing, Supervision, Funding acquisition. **Francisco Arrebola**: Methodology, Data curation, Formal analysis. **Inmaculada Ruiz Artero**: Methodology, Formal analysis. **Milagros Galisteo**: Conceptualization, Methodology, Investigation, Data curation, Formal analysis. **Pilar Aranda**: Conceptualization, Methodology, Funding acquisition. **Garyfallia Kapravelou**: Investigation, Data curation, Formal analysis. **María López-Jurado**: Conceptualization, Methodology, Writing-Original Draft, Writing-Review & Editing.

Grants

This work was supported by the Spanish Ministry of Science, Innovation and Universities [grant number RTI-2018-100934-B-I00] and the University of Granada and Junta de Andalucía through FEDER program [grant number B-AGR-662-UGR20].

Declaration of competing interest

At the time of submission, the authors have no competing interests (financial, professional or personal) that are relevant to the submitted work.

Data availability

Data will be made available on request.

Acknowledgments

The authors want to acknowledge the University of Granada, the Spanish Ministry of Science and Innovation, and the European Union through projects B-AGR-662-UGR20, RTI-2018-100934-B-I00, and the FEDER program, respectively. The funders had no role in the study design, data collection, analysis, decision to publish, or preparation of the manuscript. The special contribution to the development of the experiments by the Unidad de Experimentación Animal of CIC (Universidad de Granada) is also acknowledged.

Appendix A. Supplementary data

Supplementary data to this article can be found online at https://doi.org/10.1016/j.lfs.2023.121746.

References

[1] A. Okunogbe, R. Nugent, G. Spencer, J. Ralston, J. Wilding, Economic impacts of overweight and obesity: current and future estimates for eight countries, BMJ Glob. Health 6 (2021), e006351, https://doi.org/10.1136/bmjgh-2021-006351.

[2] R. Buettner, K.G. Parhofer, M. Woenckhaus, C.E. Wrede, L.A. Kunz-Schughart, J. Schölmerich, et al., Defining high-fat-diet rat models: metabolic and molecular effects of different fat types, J. Mol. Endocrinol. 36 (2006) 485–501, https://doi.org/10.1677/jme.1.01909.

[3] A. Hruby, J.E. Manson, L. Qi, V.S. Malik, E.B. Rimm, Q. Sun, et al., Determinants and consequences of obesity, Am. J. Public Health 106 (2016) 1656–1662, https://doi.org/10.2105/AJPH.2016.303326.

[4] M. Blüher, Obesity: global epidemiology and pathogenesis, Nat. Rev. Endocrinol. 15 (2019) 288–298, https://doi.org/10.1038/s41574-019-0176-8.

[5] L. Small, A.E. Brandon, N. Turner, G.J. Cooney, Modeling insulin resistance in rodents by alterations in diet: what have high-fat and high-calorie diets revealed? Am. J. Physiol. Endocrinol. Metab. 314 (2018) E251–E265, https://doi.org/10.1152/ajpendo.00337.2017.

[6] I.C.M. Simoes, J. Janikiewicz, J. Bauer, A. Karkucinska-Wieckowska, P. Kalinowski, A. Dobrzyń, et al., Fat and sugar—a dangerous duet. A comparative review on metabolic remodeling in rodent models of nonalcoholic fatty liver disease, Nutrients 11 (2019) 2871, https://doi.org/10.3390/nu11122871.

[7] A.L. de la Garza, A.M. Martínez-Tamez, A. Mellado-Negrete, S. Arjonilla-Becerra, G.I. Peña-Vázquez, L.M. Marín-Obispo, C. Hernández-Brenes, Characterization of the cafeteria diet as simulation of the human western diet and its impact on the lipidomic profile and gut microbiota in obese rats, Nutrients 15 (1) (2023) 86, https://doi.org/10.3390/nu15010086.

[8] A. Pezeshki, A. Fahim, P.K. Chelikani, Dietary whey and casein differentially affect energy balance, gut hormones, glucose metabolism, and taste preference in diet-induced obese rats, J. Nutr. 145 (2015) 2236–2244, https://doi.org/10.3945/jn.115.213843.

[9] R. Martínez, L.M. López-Trinidad, G. Kapravelou, F. Arrebola, M. Galisteo, P. Aranda, et al., A combined healthy strategy for successful weight loss, weight maintenance and improvement of hepatic lipid metabolism, J. Nutr. Biochem. 85 (2020), 108456, https://doi.org/10.1016/j.jnutbio.2020.108456.

[10] S. Xu, D. Hou, J. Liu, L. Ji, Age-associated changes in GSH S-transferase gene/proteins in livers of rats, Redox Rep. 23 (2018) 213–218, https://doi.org/10.1080/13510002.2018.1546985.

[11] B. Bárcena, A. Salamanca, C. Pintado, L. Mazuecos, M. Villar, E. Moltó, et al., Aging induces hepatic oxidative stress and nuclear proteomic remodelling in liver from wistar rats, Antioxidants 10 (2021) 1535, https://doi.org/10.3390/antiox10101535.

[12] A. Salamanca, B. Bárcena, C. Arribas, T. Fernández-Agulló, C. Martínez, JMa Carrascosa, et al., Aging impairs the hepatic subcellular distribution of ChREBP in response to fasting/feeding in rats: implications on hepatic steatosis, Exp. Gerontol. 69 (2015) 9–19, https://doi.org/10.1016/j.exger.2015.05.009.

[13] European Union Council, Directional on the protection of animals used for scientific purposes, Off. J. Eur. Union 276 (2010) 33–79.

[14] Carter Hubrecht, The 3Rs and humane experimental technique: implementing change, Animals 9 (2019) 754, https://doi.org/10.3390/ani9100754.

[15] J. Folch, M. Lees, G.H. Sloane Stanley, A simple method for the isolation and purification of total lipides from animal tissues, J. Biol. Chem. 226 (1957) 497–509.

[16] G. Kapravelou, R. Martínez, A.M. Andrade, C. López Chaves, M. López-Jurado, P. Aranda, et al., Improvement of the antioxidant and hypolipidaemic effects of cowpea flours (*Vigna unguiculata*) by fermentation: results of in vitro and in vivo experiments: health benefits of raw and fermented V. unguiculata, J. Sci. Food Agric. 95 (2015) 1207–1216, https://doi.org/10.1002/jsfa.6809.

[17] G. Kapravelou, R. Martínez, A.M. Andrade, E. Nebot, D. Camiletti-Moirón, V. A. Aparicio, et al., Aerobic interval exercise improves parameters of nonalcoholic fatty liver disease (NAFLD) and other alterations of metabolic syndrome in obese Zucker rats, Appl. Physiol. Nutr. Metab. 40 (2015) 1242–1252, https://doi.org/10.1139/apnm-2015-0141.

[18] D.E. Kleiner, E.M. Brunt, M. Van Natta, C. Behling, M.J. Contos, O.W. Cummings, et al., Design and validation of a histological scoring system for nonalcoholic fatty liver disease, Hepatology 41 (2005) 1313–1321, https://doi.org/10.1002/hep.20701.

[19] X. Chen, L. Li, X. Liu, R. Luo, G. Liao, L. Li, et al., Oleic acid protects saturated fatty acid mediated lipotoxicity in hepatocytes and rat of non-alcoholic steatohepatitis, Life Sci. 203 (2018) 291–304, https://doi.org/10.1016/j.lfs.2018.04.022.

[20] G. Lepage, C.C. Roy, Direct transesterification of all classes of lipids in a one-step reaction, J. Lipid Res. 27 (1986) 114–120.

[21] L. González-Torres, C. Matos, M. Vázquez-Velasco, J.A. Santos-López, I. Sánchez-Martínez, C. García-Fernández, et al., Glucomannan- and glucomannan plus spirulina-enriched pork affect liver fatty acid profile, LDL receptor expression and antioxidant status in Zucker fa/fa rats fed atherogenic diets, Food Nutr. Res. 61 (2017) 1264710, https://doi.org/10.1080/16546628.2017.1264710.

[22] S. Andrews, FastQC: a quality control tool for high throughput sequence data, Babraham Bioinformatics, 2010 (accessed September 16, 2022), https://www.bioinformatics.babraham.ac.uk/projects/fastqc/.

[23] P. Ewels, M. Magnusson, S. Lundin, M. Käller, MultiQC: summarize analysis results for multiple tools and samples in a single report, Bioinformatics 32 (2016) 3047–3048, https://doi.org/10.1093/bioinformatics/btw354.

[24] D. Kim, J.M. Paggi, C. Park, C. Bennett, S.L. Salzberg, Graph-based genome alignment and genotyping with HISAT2 and HISAT-genotype, Nat. Biotechnol. 37 (2019) 907–915, https://doi.org/10.1038/s41587-019-0201-4.

[25] H. Li, B. Handsaker, A. Wysoker, T. Fennell, J. Ruan, N. Homer, et al., The sequence alignment/map format and SAMtools, Bioinformatics 25 (2009) 2078–2079, https://doi.org/10.1093/bioinformatics/btp352.

[26] Y. Liao, G.K. Smyth, W. Shi, featureCounts: an efficient general purpose program for assigning sequence reads to genomic features, Bioinformatics 30 (2014) 923–930, https://doi.org/10.1093/bioinformatics/btt656.

[27] S. Anders, W. Huber, Differential expression analysis for sequence count data, Genome Biol. 11 (2010) R106, https://doi.org/10.1186/gb-2010-11-10-r106.

[28] M.I. Love, W. Huber, S. Anders, Moderated estimation of fold change and dispersion for RNA-seq data with DESeq2, Genome Biol. 15 (2014) 550, https://doi.org/10.1186/s13059-014-0550-8.

[29] M.D. Robinson, D.J. McCarthy, G.K. Smyth, edgeR: a Bioconductor package for differential expression analysis of digital gene expression data, Bioinformatics 26 (2010) 139–140, https://doi.org/10.1093/bioinformatics/btp616.

[30] M.J.M. Marschall, R. Ringseis, D.K. Gessner, S.M. Grundmann, E. Most, G. Wen, et al., Effect of ecdysterone on the hepatic transcriptome and lipid metabolism in lean and obese Zucker rats, Int. J. Mol. Sci. 22 (2021) 5241, https://doi.org/10.3390/ijms22105241.

[31] D.K. Gessner, A. Schwarz, S. Meyer, G. Wen, E. Most, H. Zorn, et al., Insect meal as alternative protein source exerts pronounced lipid-lowering effects in hyperlipidemic obese Zucker rats, J. Nutr. 149 (2019) 566–577, https://doi.org/10.1093/jn/nxy256.

[32] G. Cohen, M. Kim, V. Ogwu, A modified catalase assay suitable for a plate reader and for the analysis of brain cell cultures, J. Neurosci. Methods 67 (1996) 53–56.

[33] R.A. Lawrence, R.A. Sunde, G.L. Schwartz, W.G. Hoekstra, Glutathione peroxidase activity in rat lens and other tissues in relation to dietary selenium intake, Exp. Eye Res. 18 (1974) 563–569, https://doi.org/10.1016/0014-4835(74)90062-1.

[34] H. Ukeda, S. Maeda, T. Ishii, M. Sawamura, Spectrophotometric assay for superoxide dismutase based on tetrazolium salt 3′-{1-[(phenylamino)-carbonyl]-3,4-tetrazolium}-bis(4-methoxy-6-nitro)benzenesulfonic acid hydrate reduction by xanthine–xanthine oxidase, Anal. Biochem. 251 (1997) 206–209, https://doi.org/10.1006/abio.1997.2273.

[35] L. Ernster, DT diaphorase, in: Oxidation and Phosphorylation, Academic Press, 1967, pp. 309–317, https://doi.org/10.1016/0076-6879(67)10059-1.

[36] W.H. Habig, M.J. Pabst, W.B. Jakoby, Glutathione S-transferases. The first enzymatic step in mercapturic acid formation, J. Biol. Chem. 249 (1974) 7130–7139.

[37] M.M. Bradford, A rapid and sensitive method for the quantitation of microgram quantities of protein utilizing the principle of protein-dye binding, Anal. Biochem. 72 (1976) 248–254, https://doi.org/10.1016/0003-2697(76)90527-3.

[38] S.C. Woods, R.J. Seeley, P.A. Rushing, D. D'Alessio, P. Tso, A controlled high-fat diet induces an obese syndrome in rats, J. Nutr. 133 (2003) 1081–1087, https://doi.org/10.1093/jn/133.4.1081.

[39] I. Merroun, C. Sánchez-González, R. Martínez, C. López-Chaves, J.M. Porres, P. Aranda, et al., Novel effects of the cannabinoid inverse agonist AM 251 on parameters related to metabolic syndrome in obese Zucker rats, Metabolism 62 (2013) 1641–1650, https://doi.org/10.1016/j.metabol.2013.06.011.

[40] M. Conte, M. Martucci, M. Sandri, C. Franceschi, S. Salvioli, The dual role of the pervasive "fattish" tissue remodeling with age, Front. Endocrinol. 10 (2019) 114, https://doi.org/10.3389/fendo.2019.00114.

[41] S. Lasker, M.M. Rahman, F. Parvez, M. Zamila, P. Miah, K. Nahar, et al., High-fat diet-induced metabolic syndrome and oxidative stress in obese rats are ameliorated by yogurt supplementation, Sci. Rep. 9 (2019) 20026, https://doi.org/10.1038/s41598-019-56538-0.

[42] Z. Xie, H. Li, K. Wang, J. Lin, Q. Wang, G. Zhao, et al., Analysis of transcriptome and metabolome profiles alterations in fatty liver induced by high-fat diet in rat, Metabolism 59 (2010) 554–560, https://doi.org/10.1016/j.metabol.2009.08.022.

[43] M.N.B. Kristiansen, S.S. Veidal, C. Christoffersen, J. Jelsing, K.T.G. Rigbolt, Molecular characterization of microvesicular and macrovesicular steatosis shows widespread differences in metabolic pathways, Lipids 54 (2019) 109–115, https://doi.org/10.1002/lipd.12121.

[44] V.A. Piazzolla, A. Mangia, Noninvasive diagnosis of NAFLD and NASH, Cells 9 (2020) 1005, https://doi.org/10.3390/cells9041005.

[45] I.S. Idilman, I. Ozdeniz, M. Karcaaltincaba, Hepatic steatosis: etiology, patterns, and quantification, Semin Ultrasound CT MR 37 (2016) 501–510, https://doi.org/10.1053/j.sult.2016.08.003.

[46] N. Orhan Metin, A.D. Karaosmanoglu, Y. Metin, M. Karcaaltincaba, Focal hypersteatosis: a pseudolesion in patients with liver steatosis, Diagn. Interv. Radiol. 25 (2019) 14–20, https://doi.org/10.5152/dir.2018.17519.

[47] E. Unal, M.N. Ozmen, D. Akata, M. Karcaaltincaba, Imaging of aberrant left gastric vein and associated pseudolesions of segments II and III of the liver and mimickers, Diagn. Interv. Radiol. 21 (2015) 105–110, https://doi.org/10.5152/dir.2014.14360.

[48] J. Ciapaite, S.J.L. Bakker, G. Van Eikenhorst, M.J. Wagner, T. Teerlink, C. G. Schalkwijk, et al., Functioning of oxidative phosphorylation in liver mitochondria of high-fat diet fed rats, Biochim. Biophys. Acta 1772 (2007) 307–316, https://doi.org/10.1016/j.bbadis.2006.10.018.

[49] A. Ulla, M.A. Alam, B. Sikder, F.A. Sumi, M.M. Rahman, Z.F. Habib, et al., Supplementation of Syzygium cumini seed powder prevented obesity, glucose intolerance, hyperlipidemia and oxidative stress in high carbohydrate high fat diet induced obese rats, BMC Complement. Altern. Med. 17 (2017) 289, https://doi.org/10.1186/s12906-017-1799-8.

[50] O. Benard, J. Lim, P. Apontes, X. Jing, R.H. Angeletti, Y. Chi, Impact of high-fat diet on the proteome of mouse liver, J. Nutr. Biochem. 31 (2016) 10–19, https://doi.org/10.1016/j.jnutbio.2015.12.012.

[51] T.M. Penning, Aldo-keto reductase regulation by the Nrf2 system: implications for stress response, chemotherapy drug resistance, and carcinogenesis, Chem. Res. Toxicol. 30 (2017) 162–176, https://doi.org/10.1021/acs.chemrestox.6b00319.
[52] A. Di Francesco, Y. Choi, M. Bernier, Y. Zhang, A. Diaz-Ruiz, M.A. Aon, et al., NQO1 protects obese mice through improvements in glucose and lipid metabolism, NPJ Aging Mech. Dis. 6 (2020) 13, https://doi.org/10.1038/s41514-020-00051-6.
[53] S. Li, N. Eguchi, H. Lau, H. Ichii, The role of the Nrf2 signaling in obesity and insulin resistance, Int. J. Mol. Sci. 21 (2020) 6973, https://doi.org/10.3390/ijms21186973.
[54] G. Vial, H. Dubouchaud, K. Couturier, C. Cottet-Rousselle, N. Taleux, A. Athias, et al., Effects of a high-fat diet on energy metabolism and ROS production in rat liver, J. Hepatol. 54 (2011) 348–356, https://doi.org/10.1016/j.jhep.2010.06.044.
[55] N.V. Zhukova, T.P. Novgorodtseva, Y.K. Denisenko, Effect of the prolonged high-fat diet on the fatty acid metabolism in rat blood and liver, Lipids Health Dis. 13 (2014) 49, https://doi.org/10.1186/1476-511X-13-49.
[56] J. Ciapaite, N.M. van den Broek, H. te Brinke, K. Nicolay, J.A. Jeneson, S. M. Houten, et al., Differential effects of short- and long-term high-fat diet feeding on hepatic fatty acid metabolism in rats, Biochim. Biophys. Acta 1811 (2011) 441–451, https://doi.org/10.1016/j.bbalip.2011.05.005.
[57] Z. Song, A. Xiaoli, F. Yang, Regulation and metabolic significance of de novo lipogenesis in adipose tissues, Nutrients 10 (2018) 1383, https://doi.org/10.3390/nu10101383.
[58] B. Bandera Merchan, F.J. Tinahones, M. Macías-González, Commonalities in the association between PPARG and vitamin D related with obesity and carcinogenesis, PPAR Res. 2016 (2016) 1–15, https://doi.org/10.1155/2016/2308249.
[59] M. Flamment, J. Rieusset, H. Vidal, G. Simard, Y. Malthièry, B. Fromenty, et al., Regulation of hepatic mitochondrial metabolism in response to a high fat diet: a longitudinal study in rats, J. Physiol. Biochem. 68 (2012) 335–344, https://doi.org/10.1007/s13105-012-0145-3.
[60] E. Trépo, S. Romeo, J. Zucman-Rossi, P. Nahon, PNPLA3 gene in liver diseases, J. Hepatol. 65 (2016) 399–412, https://doi.org/10.1016/j.jhep.2016.03.011.
[61] D. Eberlé, B. Hegarty, P. Bossard, P. Ferré, F. Foufelle, SREBP transcription factors: master regulators of lipid homeostasis, Biochimie 86 (2004) 839–848, https://doi.org/10.1016/j.biochi.2004.09.018.
[62] Y.K. Lee, J.E. Park, M. Lee, J.P. Hardwick, Hepatic lipid homeostasis by peroxisome proliferator-activated receptor gamma 2, Liver Res. 2 (2018) 209–215, https://doi.org/10.1016/j.livres.2018.12.001.
[63] K. Takeuchi, K. Reue, Biochemistry, physiology, and genetics of GPAT, AGPAT, and lipin enzymes in triglyceride synthesis, Am. J. Physiol. Endocrinol. Metab. 296 (2009) E1195–E1209, https://doi.org/10.1152/ajpendo.90958.2008.